Electronic Supplementary Material (ESI) for Soft Matter

Supplementary Information for:

Highly stable and AC electric field-activated electrorheological fluid based on mesoporous silica-coated graphene nanosheets

Jianbo Yin*, Runtian Chang, Yan Kai and Xiaopeng Zhao*

Smart Materials Laboratory, Department of Applied Physics, Northwestern Polytechnical University, Xi'an 710129, P. R. China.

**E-mail: jbyin@nwpu.edu.cn; xpzhao@nwpu.edu.cn; Fax: 86 29 88491000; Tel: 86 29 88431662*

1. Experimental detail

Preparation of mesoporous silica-coated graphene nanosheets

First, GO was synthesized from natural graphite (Plate, Sinopharm Chemical Reagent Co. Ltd. of China) by an improved Hummers method reported by Marcano et al.[1] Then, mesoporous silica-coated GO nanosheets were prepared by the hydrolyzation of tetraethylorthosilicate (TEOS, Sinopharm Chemical Reagent Co. Ltd. of China) in surfactant-containing GO colloid.[2] Simply, as-synthesized GO (120 mg) was suspended in 200mL of aqueous solution containing 4 g of cetyltrimethyl ammonium bromide (CTAB, Sinopharm Chemical Reagent Co. Ltd. of China) and 160 mg of NaOH (Sinopharm Chemical Reagent Co. Ltd. of China) and then ultrasonically treated for 3 h. After stirring for 2 h at 40 ^{o}C, 4 g of TEOS was slowly added to the above mixture. After reaction for 12 h, the grey mesoporous silica-coated GO nanosheets were obtained by washing with boiling ethanol, separation, and drying. Finally, 1.0 g of mesoporous silica-coated GO nanosheets was dispersed into 80 mL of water containing 1.0 mL of hydrazine by ultrasonic and then heated for 2 h at 95 ^{o}C to obtained black mesoporous silica-coated graphene nanosheets. The nanosheets were filtered and further washed with water and ethanol, and then dried at 120 ^{o}C in vacuum to obtain resulting sample.

For comparison, pure mesoporous silica was also synthesized by the similar process in the absence of GO.

Characterization

The morphology was observed by scannning electron microscopy (SEM, JSM-6700F) and transmission electron microscopy (TEM, FEI Tecnai F30 G^2). The lacey support films were used for TEM measurement. The crystal structure was determined by powder

x-ray diffraction pattern (XRD, Philips X'Pert Pro). The surface composition was analyzed by X-ray photoelectron spectroscopy (XPS, Axis Ultra, Kratos) with AlK_{α} source. All binding energies were referenced to the C1s peak at 284.6 eV. The special surface area and pore size were obtained by N_2 adsorption isotherm (Nova 2000e, Quantachrome). The size distribution for pure mesoporous silica particles prepared in the absence of graphene core was analyzed by Zetasizer Nano ZS90 (Malvern).

Preparation of ER fluids

Mesoporous silica-coated graphene nanosheets or pure mesoporous silica particles were further dried at 150 ^{o}C in vacuum and then were dispersed into silicone oil (Viscosity of 50 mPa·s, density of 0.96 g/cm^3 at 25 ^{o}C) to form suspensions with a mechanical stirring and ultrasonic. The volume fraction of particles in fluid was defined by the ratio of particle volume to fluid volume. The particle density was measured by a pycnometer filled with water at room temperature. To decrease the effect of porosity on density, the pycnometer was placed in an ultrasonic cleaning bath and connected to a vacuum pump. After ultrasonic under reduced pressure for 10 min, the density was measured.

Electrorheological measurements

ER properties of fluid were measured by a stress-controlled electrorheometer (Thermal-Haake RS600) with a parallel plate system (PP ER35), DC high-voltage generator (0-10 kV)/AC high-voltage generator (0-2kV, 20-10 kHz), oil bath system (-25 -125 ^{o}C, Phoenix), and PC computer. The steady flow curves of shear stress/shear viscosity as a function of shear rate were measured by the controlled shear rate mode within 0.1 - 500 s^{-1} under various electric fields. Before each measurement, we presheared fluids for 1 min at 300 s^{-1} and then applied electric fields. The static yield

stress, which was defined as the maximum shear stress that made a solidified ER fluid start to flow, was approximately obtained with the maximum shear stress in the low shear rate region according to flow curves. In the dynamic oscillation test, the sweep test of modulus as a function of stress at a constant frequency of 1.0 Hz was initially conducted to find a linear viscoelastic region, and then the dynamic viscoelastic moduli were measured as a function of frequency at a stress in the linear viscoelastic region. The electric field was applied for 1 min prior to applying sweeping. For an equivalent comparison, the same frequency and stress were chosen for different electric fields. Each measurement was repeated three times to ensure data consistency.

Conductivity and dielectric measurements

DC conductivity of mesoporous silica-coated graphene nanosheets was measured by a two-point method on a digital high ohmmeter (Keithley 6517B). Prior to measuring, the particles were compressed into plate and then silver electrodes were deposited on both sides of plate. The conductivity of bare graphene was measured by a four-point method (RTS-8).

The dielectric spectra of fluids was measured by an impedance analyzer (HP 4284A) in the frequency range of 20 – 10^6 Hz using a measuring fixture (HP 16452A) for liquids to investigate polarization behavior. 1 V of bias electrical potential was applied to fluids during measurement. It was so small that no chain formation within fluids was induced, thus we could obtain the true behavior of interfacial polarization between particles and medium oil and then make an equitable comparison about the polarization of different materials.

Dispersion stability and wettablility measurements

Particle sedimentation test was carried out at room temperature to characterize the dispersion stability of fluids. A graduated flask was used to record the height of phase separation between the particle-rich phase and the relatively clear oil-rich phase as a function of time. The sedimentation ratio was defined by the height percentage of particle-rich phase relative to the total fluid height. The higher the sedimentation ratio was, the better the dispersion stability was.

The wettability of particles to silicone oil was measured by the Washburn method on powder contact angle analyzer (JF99A). The relative wettability of different samples was shown through the difference of curve slopes. The larger the slope was, the better the wettability was.[3]

2. SEM image of bare graphene

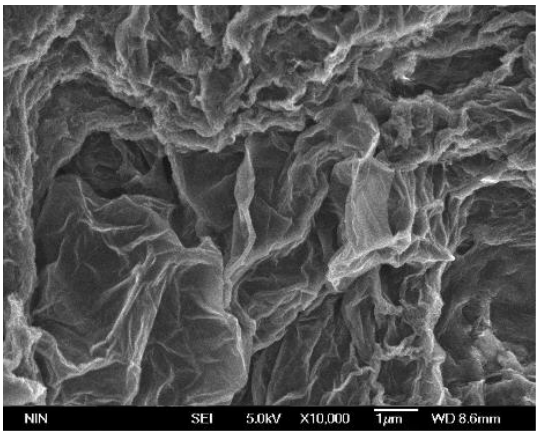

Fig. S1 SEM image of bare graphene obtained by reducing GO in hydrazine.

Fig. S1 shows that the bare graphene is easy to hold together into stacky agglomerates, which can be attributed to the strong π interaction between graphene layers

3. N_2 adsorption-desorption isotherm and pore size of mesoporous silica-coated graphene nanosheets

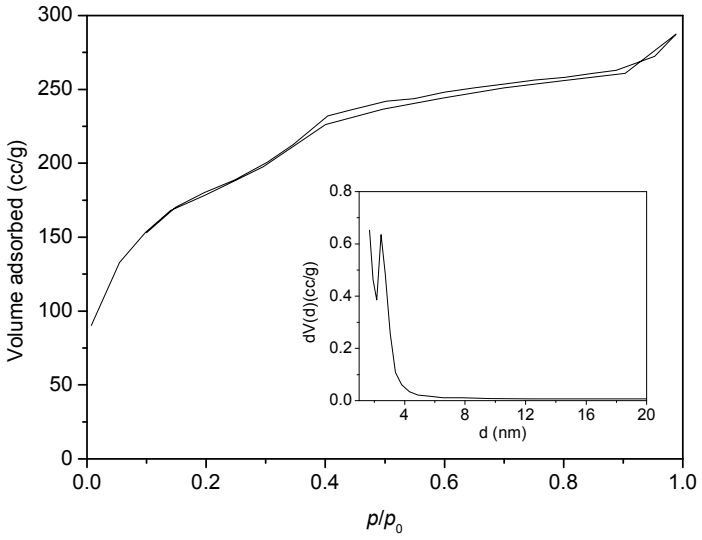

Fig. S2 N_2 adsorption-desorption isotherm of mesoporous silica-coated graphene nanosheets and corresponding pore size distribution (inset).

4. Electron diffraction and x-ray diffraction pattern comparison of bare graphene and mesoporous silica-coated graphene nanosheets

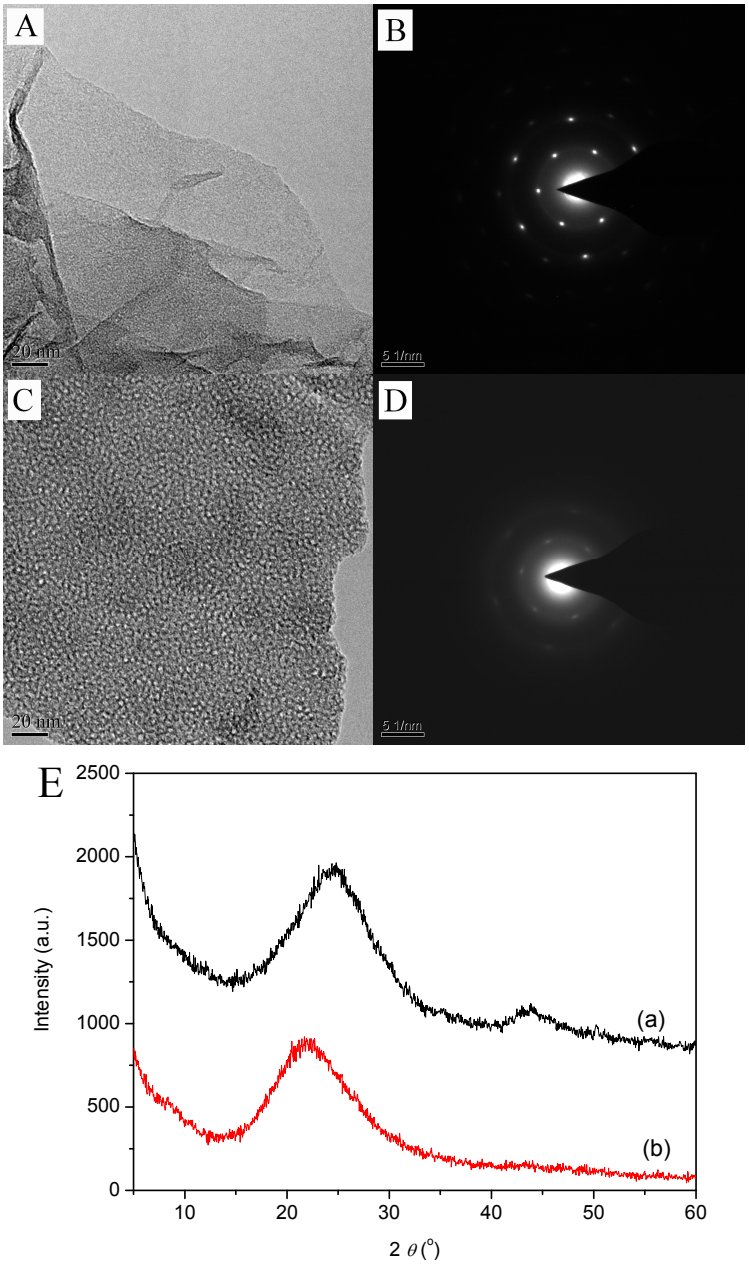

Fig. S3 TEM and corresponding ED pattern of bare graphene (A, B) and mesoporous silica-coated graphene nanosheets (C, D), XRD pattern (E) of bare graphene (a) and mesoporous silica-coated graphene nanosheets (b).

5. SEM images of mesoporous silica-coated graphene nanosheets obtained by adjusting the mass ratio of TEOS to GO in the reaction

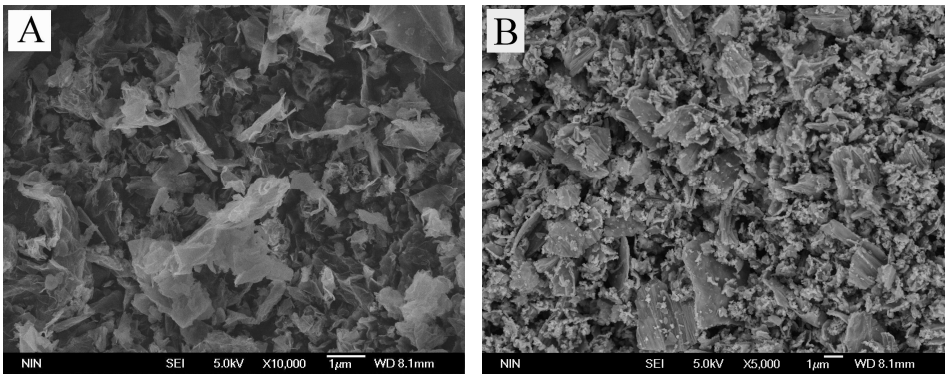

Fig. S4 SEM image of mesoporous silica-coated graphene nanosheets obtained by adjusting the mass ratio of GO/TEOS = ~0.060: 1 (A) and the mass ratio of TEOS/GO = 0.015: 1 (B).

Fig. S4 shows the SEM image of mesoporous silica-coated graphene nanosheets obtained by adjusting the mass ratio of GO/TEOS. It shows that the nanosheets are thin and easy to be re-stacking when the mass ratio of GO/TEOS is too high (~0.060: 1). When the mass ratio of GO/TEOS is too low (0.015: 1), the nanosheets become thicker but free silica particles also appear (Fig. S4B). The suitable mass ratio of GO/TEOS merits the formation of well-defined mesoporous silica-coated graphene nanosheets.

6. SEM, TEM, and particle size distribution of pure mesoporous silica obtained in the absence of GO in the reaction

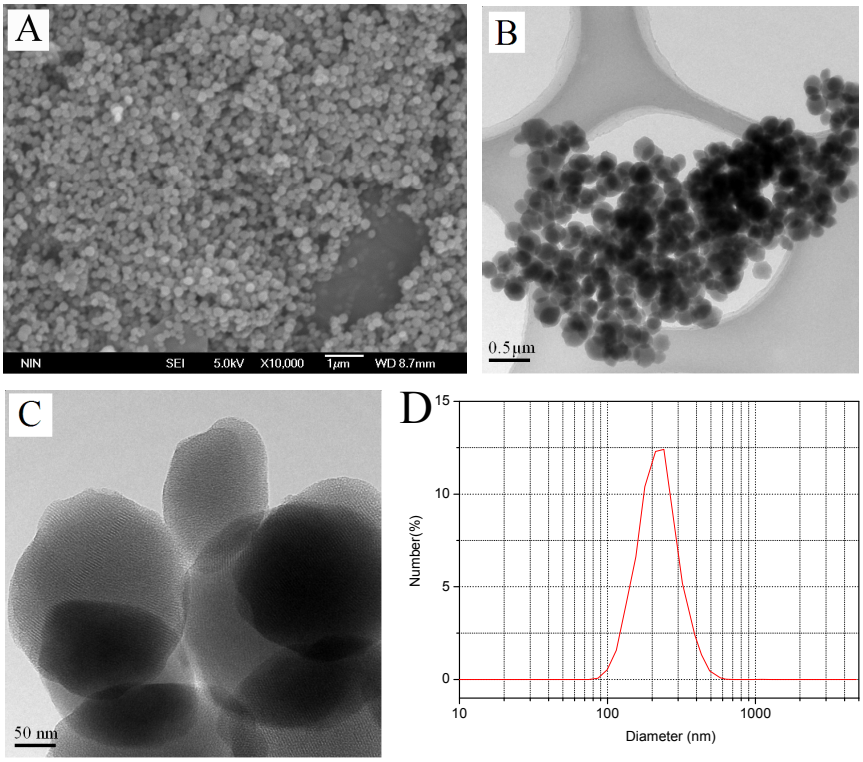

Fig. S5 SEM (A), TEM (B), high-resolution TEM (C) images, and particle size distribution of pure mesoporous silica particles.

Fig. S5 shows that, in the absence of graphene core, sphere-like pure mesoporous silica particles with a mean size of ~240 nm are obtained. The pore size measured by nitrogen physisorption measurement is 2.3 nm (not shown here), which is in accordance with the result estimated from high-resolution TEM (Fig. S5C).

7. Stress relaxation behavior of mesoporous silica-coated graphene nanosheet fluid under electric fields

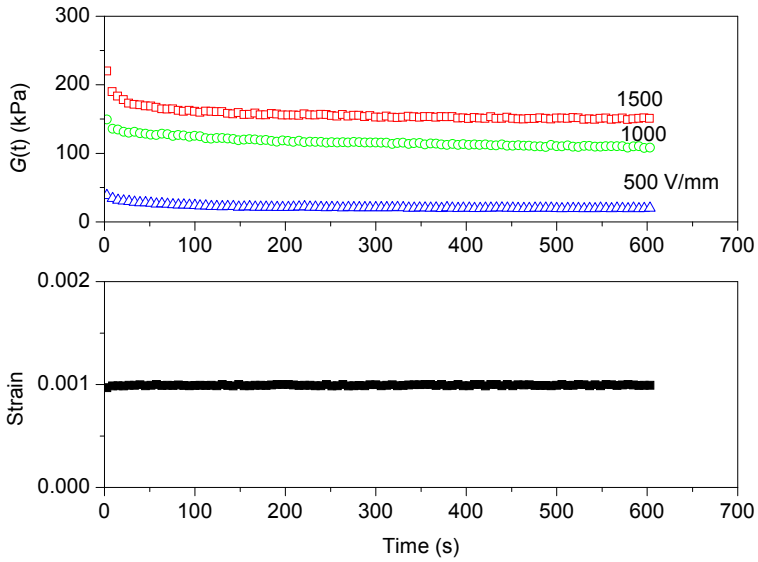

Fig. S6 Relaxation modulus (G(t)) as a function of time at constant strain (0.001) for mesoporous silica-coated graphene fluid AC electric field with frequency of 1000 Hz. (T=23 ^{o}C, particle volume fraction = 5 vol%))

8. Particle volume fraction dependence of static yield stress of mesoporous silica-coated graphene nanosheet fluid

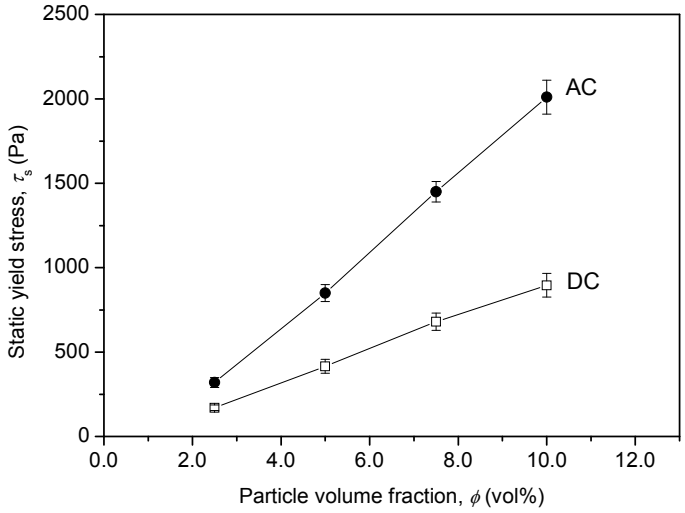

Fig. S7 Static yield stress as a function of particle volume fraction for mesoporous silica-coated graphene fluid under 1500 V/mm of DC electric field (open square symbol) and 1500 V/mm of AC electric field with frequency of 1000 Hz (solid circle symbol). (T=23 ^{o}C)

9. Dynamic viscoelastic modulus of mesoporous silica-coated graphene nanosheet fluid under electric fields

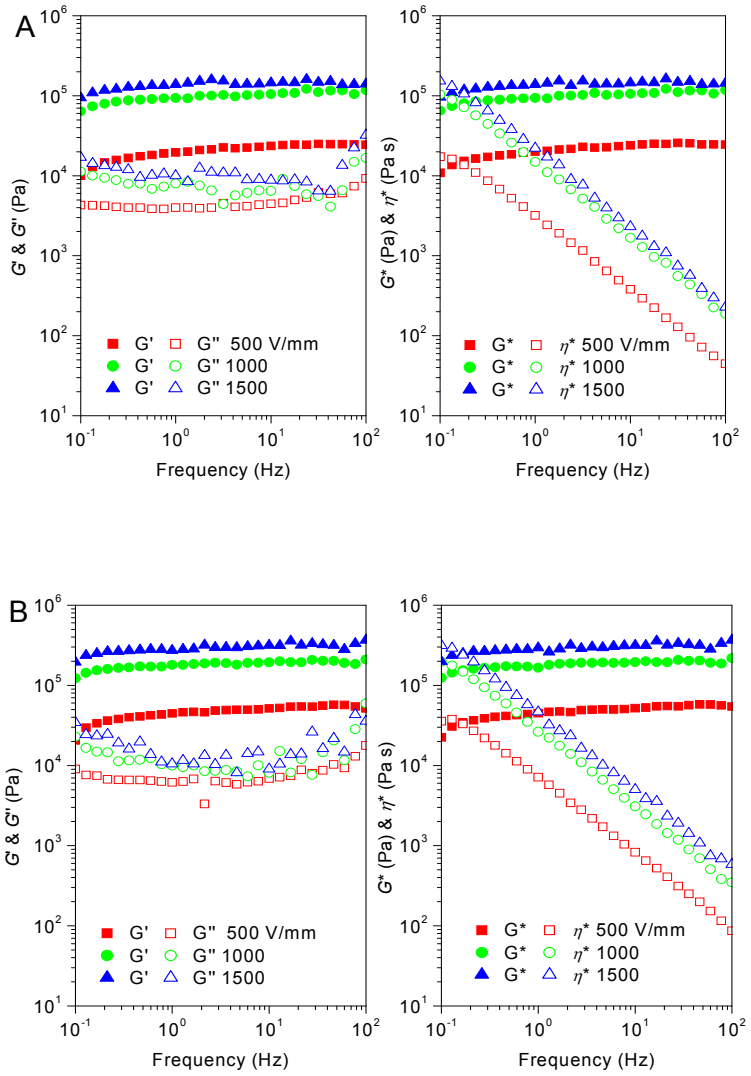

Fig. S8 Frequency dependence of dynamic shear storage modulus (G') and loss modulus (G'') (left part) and corresponding complex modulus (G^*) and complex viscosity (η^*) (right part) of mesoporous silica-coated graphene nanosheet fluid under DC electric field (A) and AC electric field with frequency of 1000 Hz (B). (T=23 ^{o}C, particle volume fraction = 5 vol%)

10. Steady shear viscosity of the pure mesoporous silica fluid under electric fields

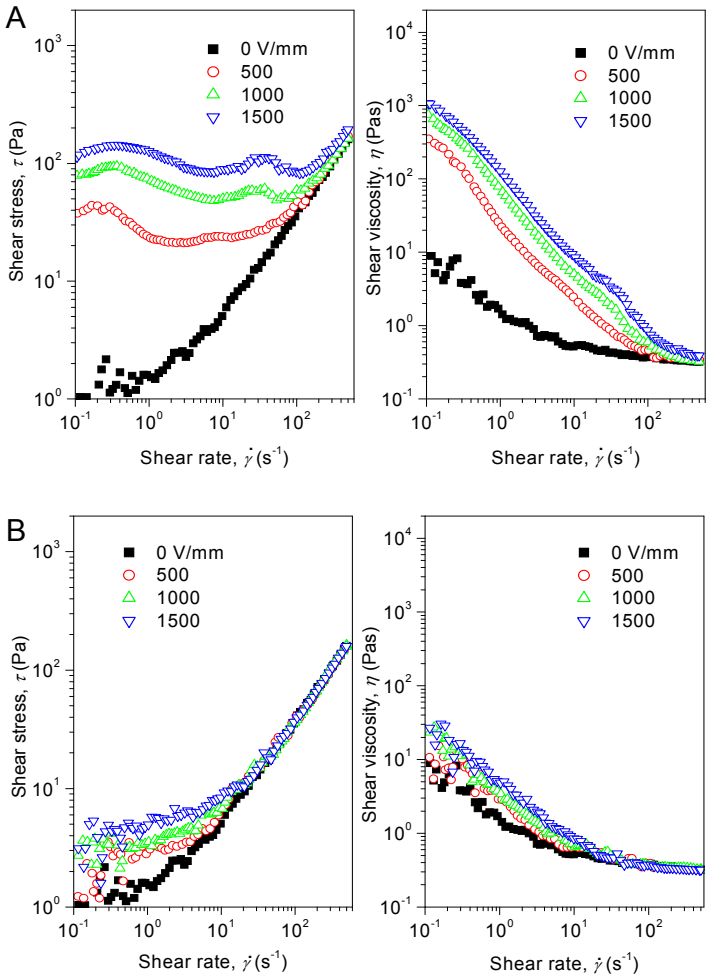

Fig. S9 Steady flow curves of shear stress (left part) and shear viscosity (right part) vs. shear rate for pure mesoporous silica fluid under DC electric field (A) and AC electric field with frequency of 1000 Hz (B). (T=23°C, particle volume fraction = 5 vol%)

11. Steady shear viscosity of the pure GO fluid under electric fields

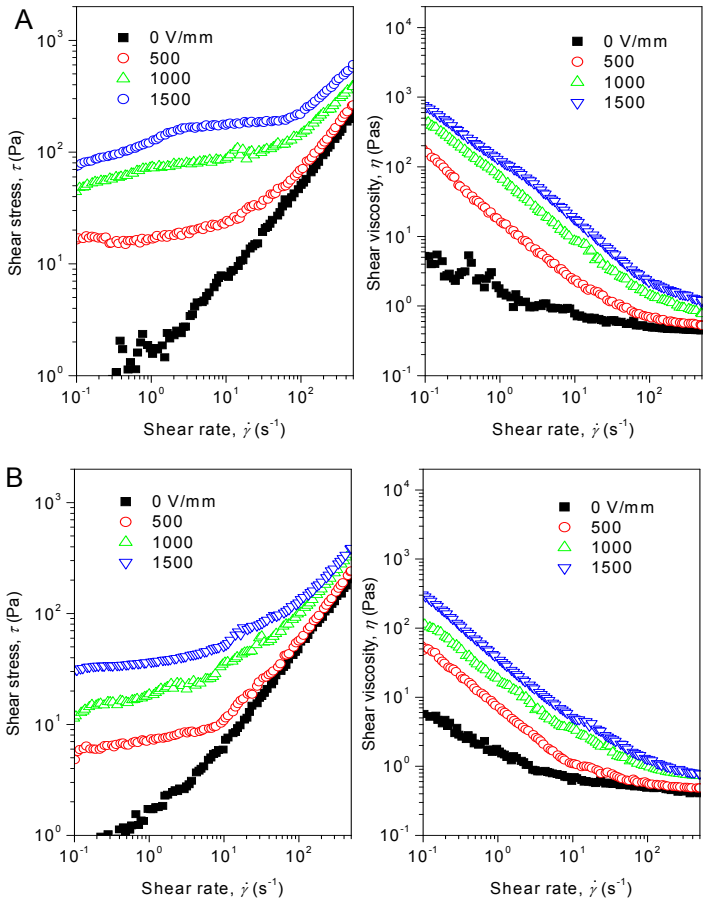

Fig. S10 Steady flow curves of shear stress (left part) and shear viscosity (right part) vs. shear rate for pure GO fluid under DC electric field (A) and AC electric field with frequency of 1000 Hz (B). (T=23°C, particle volume fraction = 5 vol%)

Dry pure GO is large-size stacking agglomerates and the fluid possesses ER response under electric fields but the ER response is lower than that of mesoporous silica-coated graphene nanosheet fluid. For example, the static yield stress of GO fluid is ~85 Pa at 1500 V/mm of DC electric field, which is lower than that (410Pa) of the latter. On exposure to AC electric field, the ER response of GO fluid decreases. For example, the yield stress decreases to ~35 Pa at 1500 V/mm and 1000 Hz of AC electric field.

12. Static yield stress of mesoporous silica-coated graphene nanosheet fluid as a function of the mass ratio of GO to TEOS in the reaction

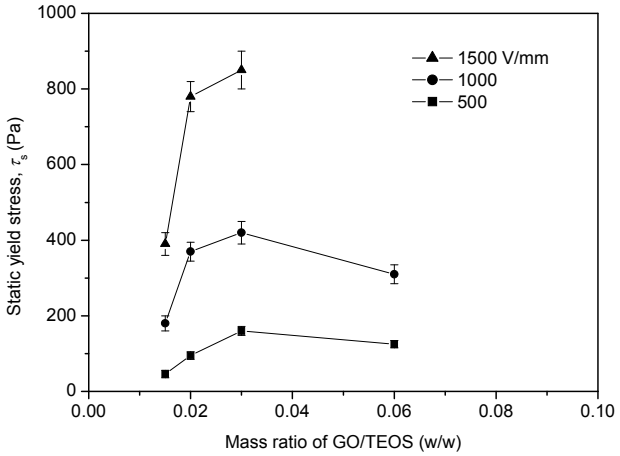

Fig. S11 Static yield stress as a function of mass ratio of GO to TEOS for mesoporous silica-coated graphene nanosheet fluid under 1000 Hz of AC electric fields. (T=23°C, particle volume fraction = 5 vol%)

13. Temperature effect of mesoporous silica-coated graphene nanosheet fluid

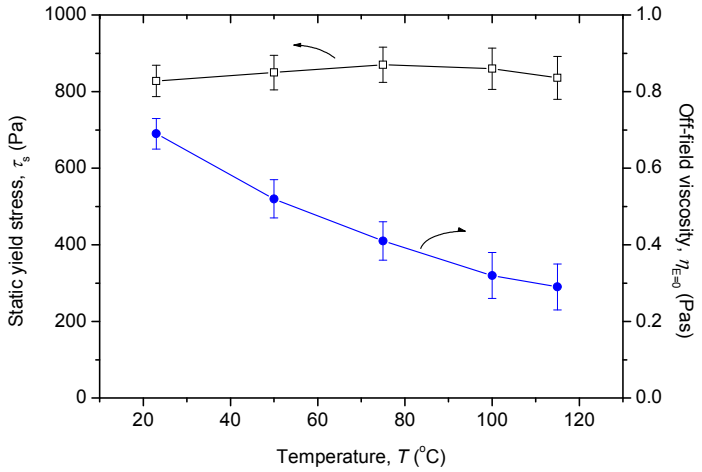

Fig. S12 Static yield stress (open square symbol, at 1500V/mm and 1000Hz of AC electric field) and off-field viscosity (solid circle symbol, determined at 500 s^{-1} of shear rate) as a function of operating temperature for mesoporous silica-coated graphene nanosheet fluid. (Particle volume fraction = 5 vol%)

14. Wetting ability comparison of bare graphene and mesoporous silica-coated graphene nanosheets in silicone oil

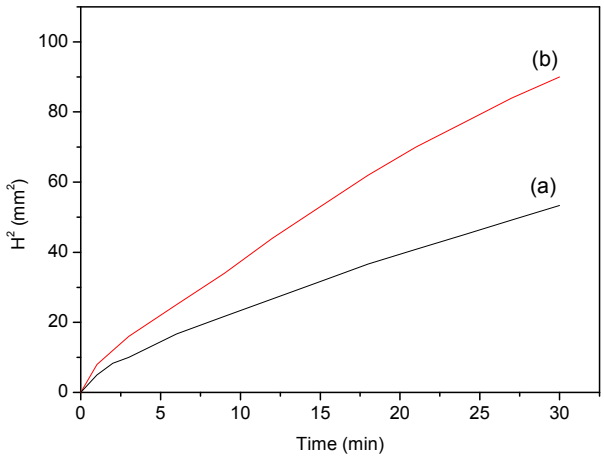

Fig. S13 Wetting curve of bare graphene (a) and mesoporous silica-coated graphene nanosheets (b) in silicone oil measured by the Washburn method. (T=23^{o}C)

15. Estimated sedimentation velocity comparison of bare graphene and mesoporous silica-coated graphene nanosheets in silicone oil

Table S1 Comparison of calculated sedimentation velocity between mesoporous silica-coated graphene nanosheets and bare graphene particles in silicone oil

	mesoporous silica-coated graphene nanosheets	bare graphene particles
Particle average radius, r (μm) [a]	~1.0	~25.0
Particle density, ρ (g/cm^3) [b]	1.86	2.05
Oil density, ρ_0 (g/cm^3) [c]	0.96	0.96
Oil viscosity, η_0 (Pa·s)[d]	0.050	0.050
Sedimentation velocity, V (m/s) [e]	~2.5×10^{-8}	~1.9×10^{-5}

[a] The average particle size was approximately determined by SEM (20 particles), [b] The particle density was measured by a pycnometer filled with water at room temperature and the detailed measurement was shown in Experimental section. [c] Silicone oil (viscosity = 50 mPas at 25 ^{o}C), [d] The sedimentation velocity was calculated by Stokes settling equation $V = kgr^2(\rho - \rho_0)/\eta_0$, where k=0.14 for plate-like mesoporous silica-coated graphene nanosheets and bare graphene particles (restacking large-size plate-like agglomerates), g gravitational acceleration. [4]

Table S1 shows that the estimated sedimentation velocity of mesoporous silica-coated graphene nanosheets is ~2.5×10^{-8} m/s for mesoporous silica-coated graphene nanosheets, which is significantly slower than that (~1.9×10^{-5} m/s) of bare graphene particles. However, it should be pointed out that the experimentally measured sedimentation velocity is much slower that the estimated sedimentation velocity by Stokes settling equation. This may be attributed to the fact that there are other reasons influencing particle sedimentation, such as the supporting effect between nanosheets.

References

1 D. Marcano, D. Kosynkin, J. Berlin, A. Sinitskii, Z. Sun, A. Slesarev, L. Alemany, W. Lu and J. Tour, *ACS Nano*, 2010, **4**, 4806.

2 S. B. Yang, X. L. Feng, L. Wang, K. Tang, J. Maier and K. Müllen, *Angew. Chem. Int. Ed.*, 2010, **49**, 4795.

3 Y. P. Qiao, J. B. Yin and X. P. Zhao, *Smart Mater. Struct.,* 2007, **16**, 332

4 J. Y. Hong and J. Jang, *Soft Matter,* 2012, **8**, 3348